Annals of Nuclear Energy 99 (2017) 58–67

Contents lists available at ScienceDirect

Annals of Nuclear Energy

journal homepage: www.elsevier.com/locate/anucene

Improvements in the prediction of heat transfer to supercritical pressure fluids by the use of algebraic heat flux models

A. Pucciarelli *, W. Ambrosini

Università di Pisa, Dipartimento di Ingegneria Civile e Industriale, Largo Lucio Lazzarino 2, 56126 Pisa, Italy

ARTICLE INFO

Article history:
Received 29 June 2016
Received in revised form 8 September 2016
Accepted 11 September 2016

ABSTRACT

The paper discusses the latest improvements obtained in performing heat transfer calculations by RANS turbulence models when dealing with fluids at supercritical pressure.

An algebraic heat flux model (AHFM) is adopted as an advanced tool for calculating the turbulent Prandtl number distribution to be used in the energy equation. Though maintaining a simple gradient approach, the proposed model manages to obtain interesting results when dealing with temperatures spanning from low to supercritical values.

This is due to the introduction of a correlation for defining one of the relevant AHFM parameters. As stated in previous works, in fact, single fixed constant values could not be sometimes sufficient for dealing with very different operating conditions such as the ones occurring with supercritical fluids. In order to make the relation suitable for different fluids, a dependence on a non-dimensional quantity which proved to be relevant by parallel work is assumed.

Some sensitivity analyses are also performed, showing some interesting capabilities in reproducing a sort of threshold behaviour when working in transition regions.

Buoyancy induced phenomena are much better captured than in past attempts, though incomplete accuracy is observed for some boundary conditions.

1. Introduction

The development of a Supercritical Water-Cooled Reactor still represents the objective of researches carried out in different Countries. In particular, a new Coordinated Research Project (CRP) started in November 2013 under the aegis of IAEA with the aim of improving the present understanding of the complex phenomena occurring when working with supercritical fluids. Support to these studies is also provided by the Generation Four International Forum (GIF), which encourages cooperation and exchanges between the various research teams.

One of the most challenging issues in the development of SCWRs is the problem of correctly predicting heat transfer deterioration and enhancement in the reactor core. In particular, heat transfer deterioration could represent a dangerous situation, since it may lead to high temperatures that could cause reactor fuel failures. Consequently, this heat transfer regime must be avoided or, at least, controlled by selecting suitable working conditions. According to Jackson and Hall (1979), heat transfer deterioration may be due to three different aspects. The most important ones are the exceeding of the so called pseudo-critical temperature, which impairs the heat transfer capabilities of the fluid, and the re-laminarization due to buoyancy effects, which reduces the turbulence in the vicinity of the wall thus impairing heat transfer.

Unfortunately, up to the present time most of the commonly used simulation techniques cannot adequately deal with this problem, reporting insufficient matching with the available experimental data: in particular, κ-ε models usually over-predict the measured trends while the κ-ω ones tend not to detect the phenomenon (Sharabi, 2008; Sharabi and Ambrosini, 2009; De Rosa, 2010; Badiali, 2011).

During the last years, researchers tried to improve the situation with new modelling proposals. Zhang et al. (2010) suggested the adoption of a four-equation turbulence model in association with the algebraic heat flux model (AHFM) for the calculation of the buoyancy production terms, reporting interesting results for a few addressed cases. The AHFM relation was firstly introduced by Launder (1987) and Launder (1988) as a steady–state algebraic simplification of the turbulent heat flux balance differential equation and allows calculating this variable without requiring the definition of a turbulent Prandtl number. However, together with the definition of four coefficients, the relation requires the calculation of the temperature variance distribution thus implying a larger

* Corresponding author.
E-mail addresses: andrea.pucciarelli@yahoo.it (A. Pucciarelli), walter.ambrosini@ing.unipi.it (W. Ambrosini).

http://dx.doi.org/10.1016/j.anucene.2016.09.022
0306-4549/

Nomenclature

Roman letters

C_t, C_{t1}, C_{t2}, C_{t3}, C_{t4}	constants of the AHFM model,-
C_p	specific Heat, J/kgK
g	gravity, m/s^2
G	mass flux, kg/m^2 s
ID	internal Diameter, m
h	enthalpy, J/kg
h^*	dimensionless Enthalpy
Pr_t	turbulent Prandtl number
q''	heat flux, W/m^2
t	time, S
$\overline{t'^2}$	temperature variance, °C^2
T	temperature, °C
T_{in}	inlet temperature, °C
T_{pc}	pseudo-critical termperature, °C
u	velocity, m/s
u_x	axial velocity, m/s
v	radial velocity, m/s
x	axial position, m
$y+$	dimensionless distance from the wall, –

Greek letters

β	isobaric thermal expansion coefficient, 1/K
ε	turbulent dissipation rate, m^2/s^3
ε_t	dissipation rate of $\overline{t'^2}$, K^2/s
κ	turbulent kinetic energy, m^2/s^2
ν_t	eddy viscosity, m^2/s

Subscripts

pc	pseudo-critical temperature
w	wall

Abbreviations

AHFM	algebraic heat flux model
AKN	Abe Kondoh Nagano (turbulence model)
RANS	Reynolds averaged Navier Stokes
SCWR	supercritical water-cooled reactor
SGDH	simple gradient diffusion hypothesis

computational cost by introducing two additional partial differential equation for this variable and its dissipation.

The research team in Pisa considered interesting this suggestion in the frame of latest works (Pucciarelli, 2013; Borroni, 2014; Pucciarelli et al. 2015) trying to assess the capabilities of this technique. The adoption of the AHFM for the buoyancy terms, while keeping the typical Simple Gradient Hypothesis for the energy equation, allowed some improvements, but problems still appeared when approaching the pseudo-critical temperature. As a natural subsequent step, the adoption of AHFM even in the energy equation was considered.

A similar path was also followed by Xiong and Cheng (2014) who, adopting an Elliptical Blending-AHFM relation in association with the κ-ε-ζ-f turbulence model, reported good coherence between the obtained RANS calculations and a selected reference DNS data set. The research team in Pisa decided to investigate a wider spectrum of experimental data; the calculations were performed adopting the Lien κ-ε model (Lien et al., 1996) as implemented in CD-adapco's STAR-CCM+ (CD-adapco, 2015), because of the good experience achieved in the frame of previous works with this model (Ambrosini et al., 2015). Due to obvious restrictions in the access to the internal structure of a commercial code, it was not possible directly using AHFM for calculating the turbulent heat fluxes in the energy equation, limiting the developments to the use of what is manageable with field functions; as a consequence, AHFM was used for obtaining a relation providing a more reliable turbulent Prandtl number distribution in an isotropic approach to turbulent heat transfer in the energy equation, as an improvement with respect to keeping it equal to a fixed constant value.

This attempt (Pucciarelli et al., 2016) showed that the introduction of AHFM in the energy equation can really improve the obtained results with respect to the previous state-of-the art; nevertheless, it reported wall temperature underestimations for cases considering large pipes and downward flow conditions. A new set of coefficients for AHFM was proposed in the frame of this work; nevertheless, the final results showed that a single set of parameters was not sufficient for describing the complicated involved phenomena in all the addressed conditions.

The aim of the present work is improving the results obtained in last experiences, by introducing a relation defining the value of one of the relevant AHFM coefficients. Thus, a further degree of freedom is removed from the model which, as a consequence, should be capable to autonomously adapt to different flow and boundary conditions providing better results.

2. Adopted model

As in the previous works, the commercial code STAR-CCM+ is adopted for the present calculations, trying to improve the model proposed in the paper Pucciarelli et al. (2016). The Lien κ-ε (Lien et al., 1996) turbulence model in association with a low y+ approach is still used; as in the previous work, a further scalar equation for the temperature variance as proposed by Abe et al. (1994,1995) and an algebraic relation for the calculation of its dissipation rate are introduced for allowing adopting the AHFM model. For further information about the various assumptions, the reader is referred to the paper Pucciarelli et al. (2016).

As anticipated, AHFM expression by Launder requires the turbulence variance distribution for being adopted, since it appears in the last term of the relation which is reported below in the form proposed by Zhang et al. (2010):

$$\overline{u_i't'} = -C_t \frac{\kappa}{\varepsilon}\left[C_{t1}\overline{u_i'u_j'}\frac{\partial \mathrm{T}}{\partial x_j} + (1-C_{t2})\overline{u_j't'}\frac{\partial \overline{u}_i}{\partial x_j} + (1-C_{t3})\beta g_i \overline{t'^2}\right] \quad (1)$$

This relation also requires the definition of a set of four parameters whose values cannot be completely inferred by theory: different proposals were formulated in the past years for these parameters but there is no particular agreement among the various Authors (see, e.g., Kenjereš et al., 2005; Zhang et al., 2010; Shams et al., 2014). In fact, the optimization of the set of these parameters seems to be strongly dependent on both the turbulence model adopted as a basis for the analysis and the considered operating conditions. A good optimization for supercritical fluids in fact may not fit for liquid metals applications. This behaviour was noticed in a previous paper by Pucciarelli et al. (2016), where four different sets of parameters were taken into account reporting relevant differences in the obtained results.

Though interesting results were obtained with the set of parameters proposed in that paper, from now on renamed as 2016-Ht, a new one was introduced in the frame of a parallel work regarding fluid to fluid scaling (Pucciarelli and Ambrosini, 2016), from now

on renamed as 2016-Sc; both the considered sets are reported below:

$$Set\ 2016-Ht: C_t = \frac{2}{3};\ C_{t1} = 1;\ C_{t2} = 0.4,\ C_{t3} = 0.18 \tag{2}$$

$$Set\ 2016-Sc: C_t = 1;\ C_{t1} = 0.113;\ 1 - C_{t2} = 0.113;\ 1 - C_{t3} = 1.5 \tag{3}$$

As it can be seen from Eq. (3), in the latest paper some of the AHFM parameters were defined through the complement to one of the coefficients reported in Eq. (1). The main advantage of this choice is that the global coefficient of each contribution is directly provided and it is easier to understand the real weight of each term in respect to the global balance. The same definitions are considered also in the present paper since, as explained below, the last AHFM component will be assumed to be variable and adopting such a definition will improve both readability and comprehension.

The two sets tend to produce very similar results, nevertheless the main advantage in adopting the 2016-Sc set, is that it is more coherent with the other assumption of the proposed model regarding the definition of the turbulent Prandtl number:

$$\mathrm{Pr_t} = -\frac{\nu_t}{\overline{u_r' t'}} \cdot \frac{\partial \mathrm{T}}{\partial \mathrm{r}} \tag{4}$$

The above relation assumes that the most relevant direction for calculating a good estimation of the turbulent Prandtl number is the one perpendicular to the wall, i.e., the radial one rather than the axial one for 2D pipe geometries; the velocity-temperature fluctuation correlation appearing in this relation is calculated adopting the above reported AHFM expression. While the 2016-Sc set is suitable for using AHFM both for the calculation of $\mathrm{Pr_t}$ and the production term of turbulence due to buoyancy, the one from the previous paper required two different values of the C_t parameter. As a consequence the 2016-Sc set is used as a reference for the proposed improvements in the present work except for the last term, $(1 - C_{t3})$, which, coherently with the idea which is the leitmotiv of this paper, is no more kept constant but it is obtained by a relation taking into account the wall conditions, as explained later on.

As stated in both the previously mentioned papers, the proposed set of parameters were able at dealing with different experimental conditions, though they tended at underestimating the wall temperature trend when facing large pipes. In these cases, better results could be obtained varying some of the parameters and, in particular, imposing $1 - C_{t3} = 0$ for the 2016-Sc set as shown in Figs. 1 and 2. Nevertheless, the same choice would have deleterious effects in other cases, such as the ones proposed in Figs. 3 and 4. As a rule of thumb, it was noticed that lower values of $1 - C_{t3}$, close to zero, were usually suitable for wall temperatures lower than the pseudo-critical temperature while higher values were needed for temperature values that exceeded that threshold.

As a consequence, the idea that a fixed constant value could be sufficient for dealing with very different experimental conditions was discarded, preferring a dynamic definition of the coefficient as a result of an empirical relation to be attentively selected. Different attempts were performed taking into account different fluid properties and flow boundary conditions, but in the end we found that good results could be obtained by using a relation depending just on the dimensionless enthalpy h^*.

This dimensionless enthalpy represents a dimensionless distance of the current conditions from the pseudo-critical ones and was firstly introduced by Ambrosini and Sharabi (2008) for stability analyses in heated channels containing supercritical pressure fluids. It is defined as

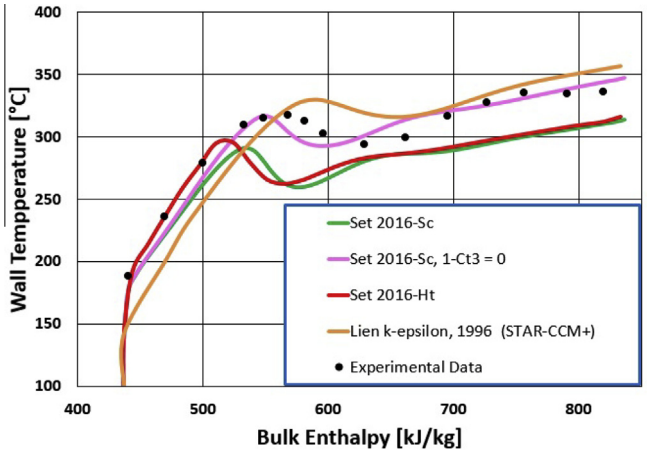

Fig. 1. Data by Pis'menny et al. (2005a,b). Water, 23.5 MPa, 9.5 mm ID, Tin = 100 °C, G = 248 kg/m^{2}s, q″ = 396 kW/m^2.

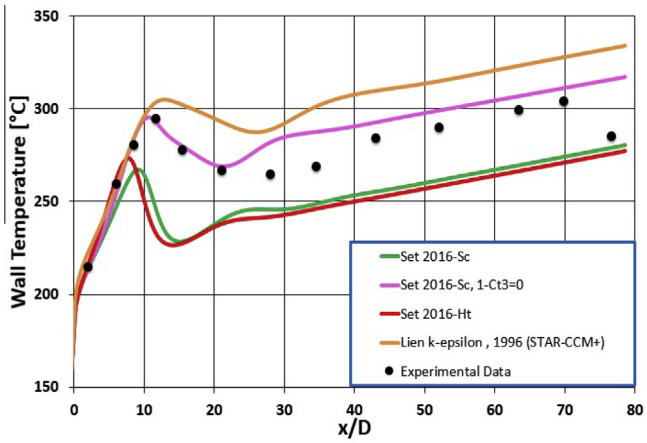

Fig. 2. Data by Watts (1980). Water, 25 MPa, 24.5 mm ID, Tin = 150 °C, G = 273 kg/m^2 s, q″ = 250 kW/m^2.

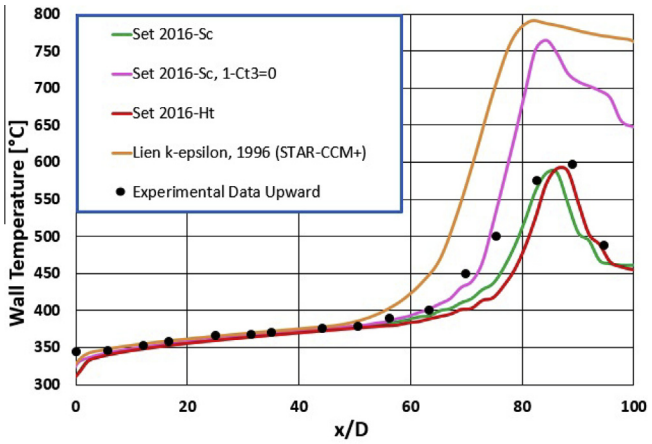

Fig. 3. Data by Pis'menny et al. (2005a,b). Water, 23.5 MPa, 6.28 mm ID, Tin = 300 °C, G = 508 kg/m^2 s, q″ = 390 kW/m^2.

$$h^* = \frac{\beta_{pc}}{C_{p,pc}}(h - h_{pc}) \tag{5}$$

where the subscript "pc" means that the relative quantity is calculated at the pseudo-critical temperature. As reported in Pucciarelli

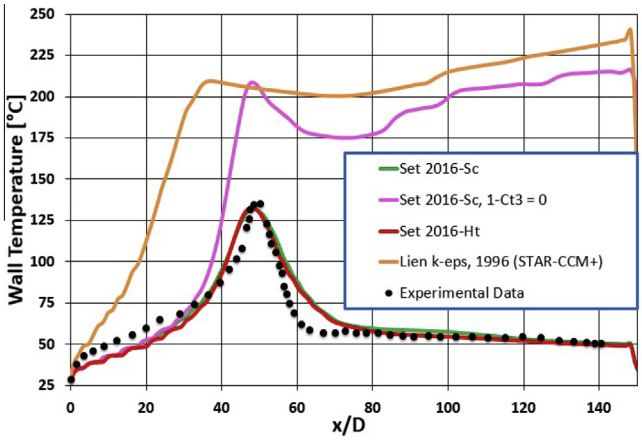

Fig. 4. Data by Fewster (1976): CO_2, 7.584 MPa, 5.1 mm ID, Tin = 20 °C, G = 631.48 kg/(m^2 s), q″ = 68 kW/m^2.

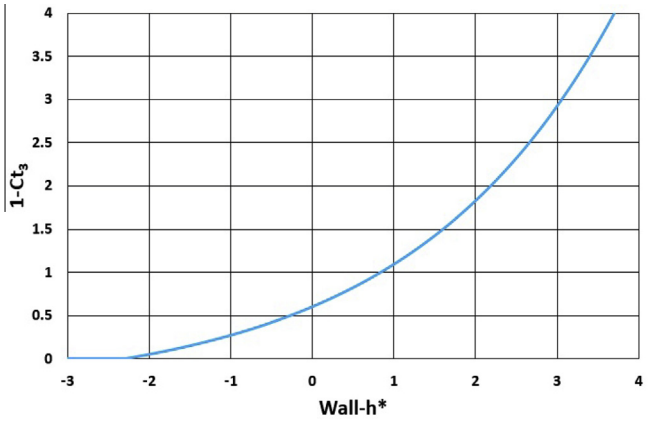

Fig. 6. Obtained trend when adopting the proposed relation for the calculation of 1-C_{t3}.

and Ambrosini (2016), (to which the reader is referred for further information) the concept of h^* seems very important for performing fluid-to-fluid scaling since, as reported in Fig. 5, it allows comparing experimental conditions obtained with different fluids in a very effective way.

As a consequence, the dimensionless enthalpy was used as the independent parameter for the calculation of the C_{t3} parameter in the following empirical relation, found after a number of trials, being convinced that it could have a similar general value even for this application:

$$C_{t4} = 1 - C_{t3} = Max\left(0, e^{\frac{h^*_w}{2.5}} - 0.4\right) \quad (6)$$

where the subscript "w" means that the dimensionless enthalpy is calculated at the wall. The trend of the obtained parameter is reported in Fig. 6; note that the value $h^* = 0$ corresponds exactly to the pseudo-critical temperature.

For sake of completeness, the set of parameters adopted in the present work is reported below and it will be labelled as "Present Set" in the next section reporting the obtained results.

$$Present\ Set: C_t = 1;\ C_{t1} = 0.113;\ 1 - C_{t2} = 0.113;$$
$$C_{t4} = 1 - C_{t3} = \text{Eq. (6)} \quad (7)$$

3. Obtained results

The present section reports the comparison between the latest results and the ones obtained in past analyses; comparisons with calculations adopting different values of the $C_{t4} = 1 - C_{t3}$ parameter are present as well. Figs. 7 and 8 report the results obtained for the same conditions considered in Figs. 3 and 4 respectively. As it can be noted, the present set is able at reproducing quite correctly the measured trends returning results very similar to the ones obtained in the frame of the two previous papers considering AHFM in the energy equation (Pucciarelli et al., 2016; Pucciarelli and Ambrosini, 2016). Results obtained in previous analyses adopting two-equation turbulence models are omitted in order to make the picture clearer; in fact, as shown by the prediction obtained in Figs. 3 and 4 by the Lien κ-ε (Lien et al., 1996) turbulence model, such models tended to strongly overestimate the measured wall temperature. So, even if there is no particular improvement in comparison to the authors' latest works, the obtained good coherence with the experimental data still is a very important feature for the "Present set" since it returns considerably better predictions than the ones obtained with commonly used turbulence models.

Figs. 9 and 10 report two further comparisons concerning supercritical CO_2. In these two cases, promising results were obtained even when using the 2016-Sc set; nevertheless, in particular for the case in Fig. 9, the trend obtained by this previous set resulted in an underestimation of the experimental data. This case represents one of the situations in which the selected C_{t4} parameter for set 2016-Sc is too large returning, as a consequence, lower temperatures. In fact, the last term of the AHFM relation (Eq. (1)) is always negative for upward flow cases, resulting in a positive contribution for the turbulent heat flux. As a consequence,

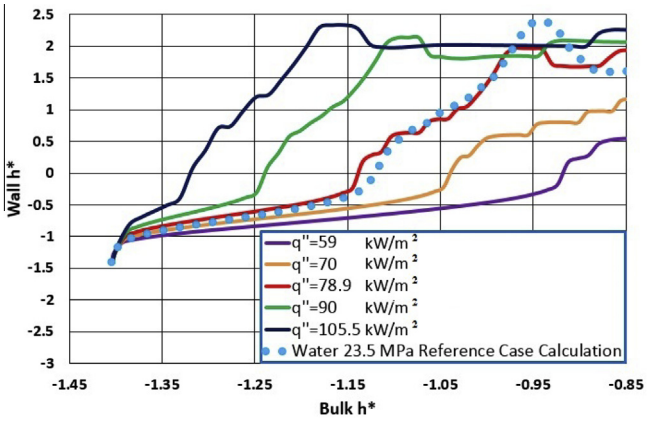

Fig. 5. Data by Pis'menny et al. (2005a,b). Water, 23.5 MPa, 6.28 mm ID, Tin = 300 °C, G = 508 kg/m^2 s, q″ = 390 kW/m^2, scaling attempts by using CO_2 at 7.584 MPa.

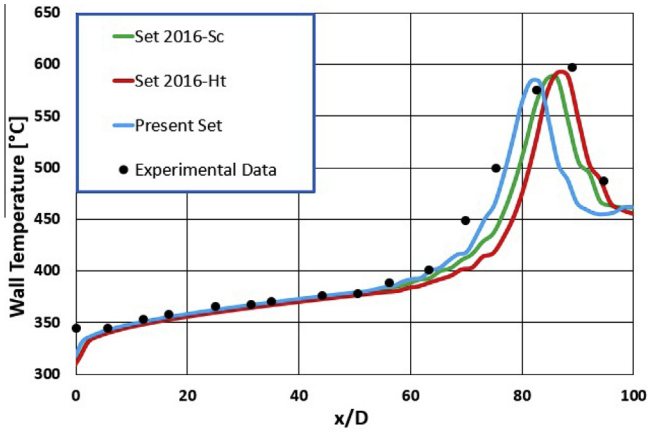

Fig. 7. Data by Pis'menny et al. (2005a,b). Water, 23.5 MPa, 6.28 mm ID, Tin = 300 °C, G = 508 kg/m^2 s, q″ = 390 kW/m^2.

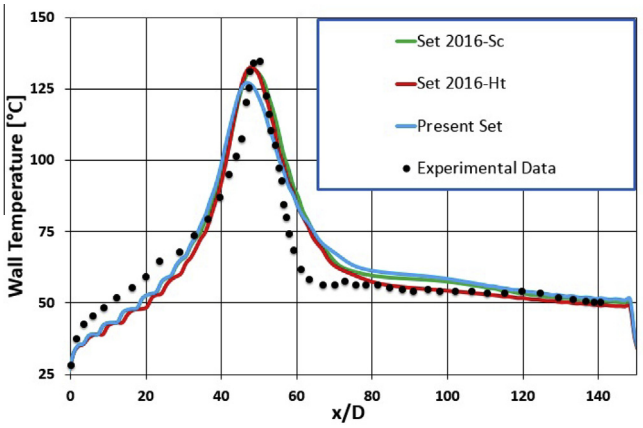

Fig. 8. Data by Fewster (1976): CO_2, 7.584 MPa, 5.1 mm ID, Tin = 20 °C, G = 631.48 kg/(m^2 s), q″ = 68 kW/m^2.

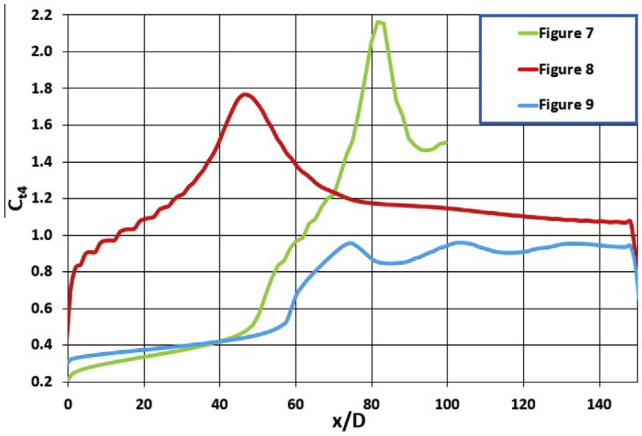

Fig. 11. Obtained C_{t4} trend for some of the addressed cases.

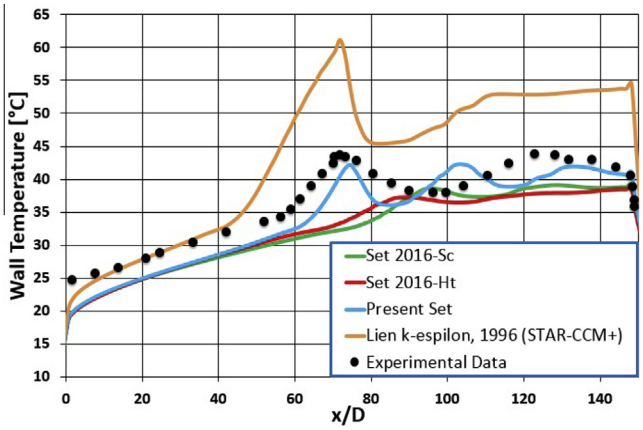

Fig. 9. Data by Fewster (1976). CO_2, 7.584 MPa, 5.1 mm ID, Tin = 11.5 °C, G = 283 kg/(m^2 s), q″ = 17.7 kW/m^2.

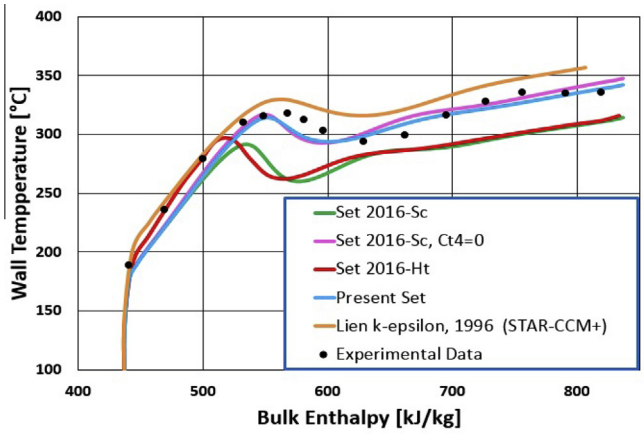

Fig. 12. Data by Pis'menny et al. (2005a,b). Water, 23.5 MPa, 9.5 mm ID, Tin = 100 °C, G = 248 kg/m^2 s, q″ = 396 kW/m^2.

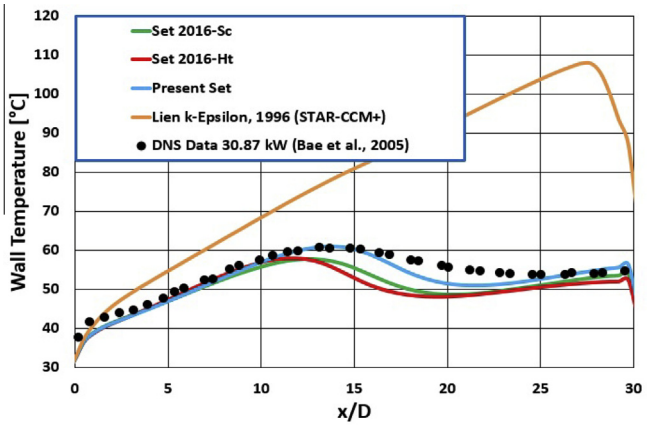

Fig. 10. DNS Data by Bae et al. (2005). CO_2, 8 MPa, 2 mm ID, Tin 28 °C, Rein = 5400, q″ = 30.87 kW/m^2.

selecting a large value for C_{t4}, implies higher turbulent heat flux values and improved buoyancy turbulence production which, in turn, results in low wall temperature trends.

The present set, thanks to its dynamic definition of the C_{t4} parameter, whose trend is reported in Fig. 11, allows for obtaining better coherence with experimental data. Results obtained in the past with two equation turbulence models, such as Lien κ-ε (Lien et al., 1996), resulted once again in strong overestimations of the wall temperature due to the exceeding of the pseudo-critical temperature. Fig. 11 also reports the trends of C_{t4} parameter obtained for the cases in Figs. 7 and 8. As it can be noted the calculated values are very different, spanning from the average value of 0.9 for Fig. 11 to the peaks up to 2.2 for the case in Fig. 7; consequently, selecting only a fixed value for the considered parameter would turn out to be very limiting. Concerning Fig. 10, the "Present set" slightly refines the interesting features obtained by the sets proposed in previous papers (Pucciarelli et al., 2016; Pucciarelli and Ambrosini, 2016) resulting in strong improvements if compared with previous results.

These results were obtained for relatively small pipes; as already mentioned, moving to pipes with larger diameters, the sets adopted in the two previous papers started to underestimate the measured wall temperature trend. Fig. 12 reports the first proposed comparison, considering a 9.5 mm diameter pipe in conditions well below the pseudo-critical temperature. As it can be noticed, both the 2016-Sc and 2016-Ht Sets, returned wall temperature underestimations of about 50 degrees. Better results may be obtained both imposing $C_{t4} = 1 - C_{t3} = 0$ or adopting simpler turbulence models; in particular, the Lien κ-ε (Lien et al., 1996) turbulence model here reports a good performance since the pseudo-critical temperature in not exceeded. The "Present set" reports a good performance, comparable to the one obtained imposing $C_{t4} = 0$ which is a sort of optimized value for the presently selected case.

Fig. 13 reports the results obtained for a case considering conditions well below the pseudo-critical temperature. As mentioned above, in these cases the Lien κ-ε (Lien et al., 1996) turbulence model manages to return reasonable results, both the sets 2016-Sc and 2016-Ht instead report underestimation predicting a weak heat transfer deterioration phenomenon. Adopting the "Present set" very good coherence can be now achieved; comparing the calculated average C_{t4} parameter shown in Fig. 18 with the fixed value of 1.5 selected for set 2016-Sc, it is clear that in the past setting the chosen value was too large, resulting in wall temperature trend underestimations. Fig. 14 shows results for a case considering slightly more difficult conditions, since the heat flux is increased in comparison to the previous case but the pseudo-critical temperature is not exceeded yet. The experimental data report heat transfer deterioration and recovery; nevertheless, the Lien κ-ε (Lien et al., 1996) turbulence model can only predict the former, thus failing with the latter. Failure was reported even for the 2016-Sc and 2016-Ht sets; once more underestimation occurs because of the selected C_{t4} parameter. The "Present set" reports instead again a good performance, heat transfer deterioration occurs later and recovery earlier than in the experimental data, but the overall prediction shows good coherence both from the qualitative and quantitative point of view.

Similar behaviours can be noticed even for the case in Fig. 15 where wall temperature also exceeds the pseudo-critical threshold. In proximity of the point in which wall temperature is exceeding the pseudo-critical one (T_{pc} = 384.9 °C), the Lien κ-ε (Lien et al., 1996) turbulence model reports a strong temperature increase due to the degradation of the thermodynamic properties of the fluid and the poor turbulence conditions, something not occurring in the experimental data. The "Present set" instead, though exceeding the pseudo-critical temperature too, does not report such an overestimation, correctly reproducing a heat transfer recovery. Fig. 16 also reports similar experimental conditions; nevertheless, in this case the "Present set" still reports underestimation, though the prediction is definitely improved in comparison to previous results obtained adopting two equation turbulence models which, depending on their approach, κ-ε or κ-ω, tended to overestimate heat transfer deterioration or not predicting it at all respectively. Some sensitivity analyses were performed concerning this experimental condition and will be reported in the next section.

Finally, Fig. 17 reports a case where no heat transfer deterioration was noted from the experimental measurements, because of the imposed larger mass flux; Fig. 18 than reports the trends of the parameter C_{t4} for the above addressed cases. Once again, though normal heat transfer conditions occur upstream, when the pseudo-critical temperature is reached at the wall region, the Lien κ-ε (Lien et al., 1996) turbulence model reports a strong temperature peak. The "Present set" instead reports a better prediction, the general trend is reproduced both qualitatively and quantitative though the predicted heat transfer recovery phenomenon occurs to be larger and earlier in comparison to the experimental data.

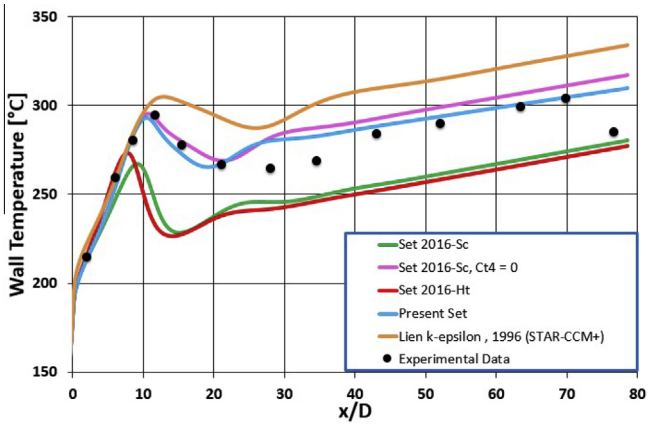

Fig. 13. Data by Watts (1980). Water, 25 MPa, 24.5 mm ID, Tin = 150 °C, G = 273 kg/m^2 s, q″ = 250 kW/m^2.

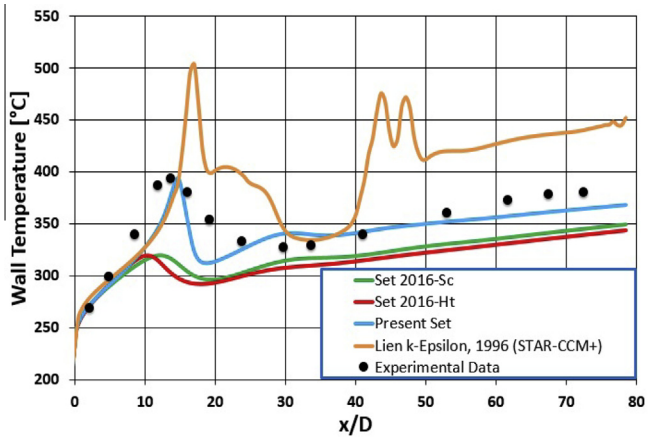

Fig. 15. Data by Watts (1980). Water, 25 MPa, 24.5 mm ID, Tin = 200 °C, G = 392 kg/m^2 s, q″ = 400 kW/m^2.

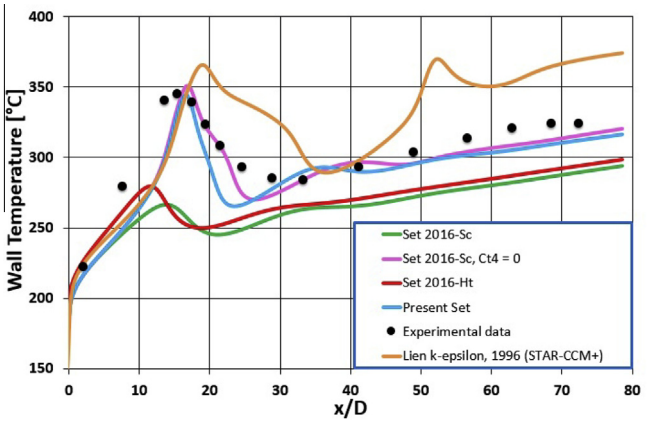

Fig. 14. Data by Watts (1980). Water, 25 MPa, 24.5 mm ID, Tin = 150 °C, G = 364 kg/m^2 s, q″ = 340 kW/m^2.

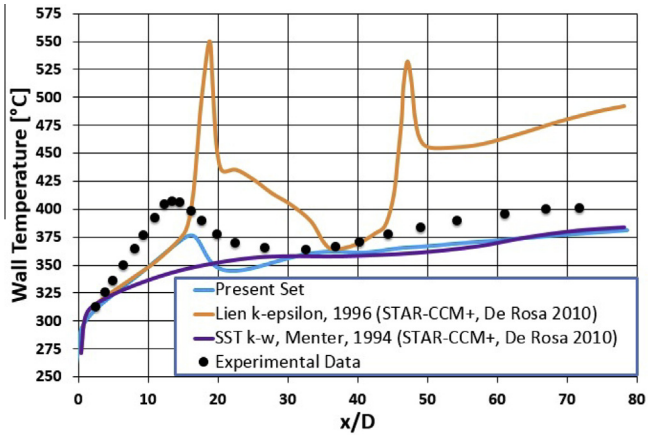

Fig. 16. Data by Watts (1980). Water, 25 MPa, 24.5 mm ID, Tin = 250 °C, G = 392 kg/m^2 s, q″ = 340 kW/m^2.

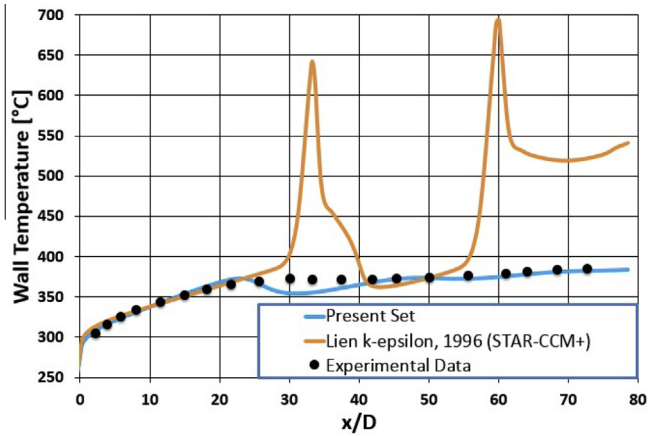

Fig. 17. Data by Watts (1980). Water, 25 MPa, 24.5 mm ID, Tin = 250 °C, G = 477 kg/m^2 s, q″ = 400 kW/m^2.

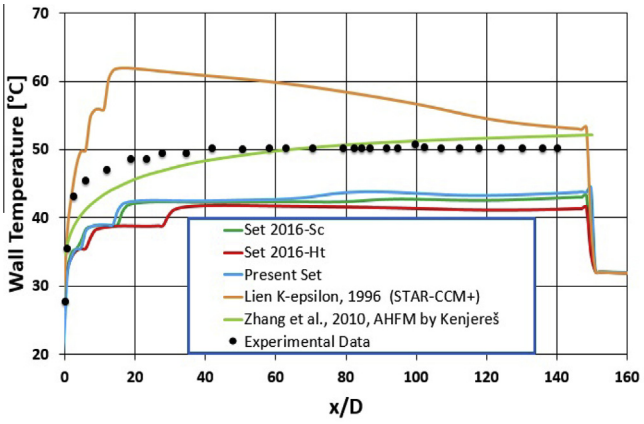

Fig. 20. Data by Fewster (1976): CO_2, 7.584 MPa, 5.1 mm ID, Tin = 20 °C, G = 631.48 kg/(m^2 s), q″ = 68 kW/m^2, Downward flow.

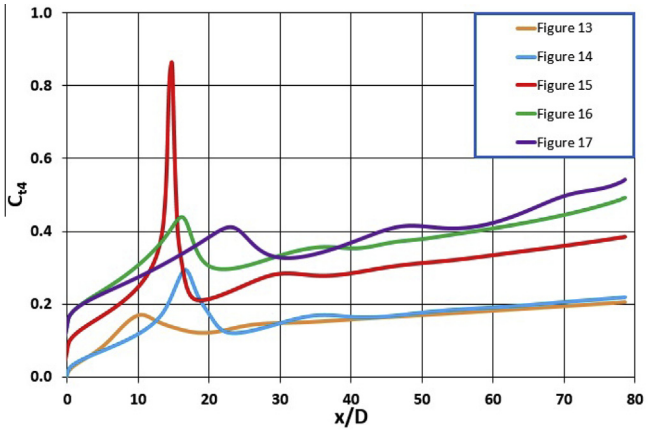

Fig. 18. Obtained C_{t4} trend for the addressed cases.

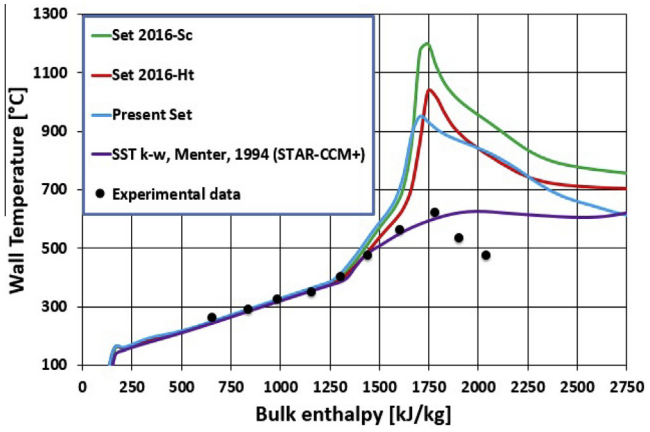

Fig. 19. Data by Ornatsky and Glushchenko (1971): Water, 25.5 MPa, 3.0 mm ID, Tin = 300 K, G = 1500 kg/(m^2 s), q″ = 1810 kW/m^2.

Figs. 19 and 20 report instead two sample cases where the "Present set" still fails. Fig. 19 shows the results obtained for one of the experimental data by Ornatsky and Glushchenko (1971); a large mass flux is imposed in this case, so that buoyancy is no more responsible for the observed heat transfer deterioration phenomena, which in this case are probably due to a combination of flow acceleration and wall temperature exceeding the pseudo-critical value. In addition, both wall and bulk temperature exceed the pseudo-critical value thus implying strong property changes and making the operating conditions very challenging. As it can be noted, lots of the selected models and settings report overestimation of the measured trend; the ones adopting AHFM in the energy equation show somewhat improvements with respect to the Lien κ-ε (Lien et al., 1996) turbulence model (Temperature peak over 2000 °C, here not shown), but the quality still remains insufficient. Adopting the SST κ-ω (Menter, 1994) may sometimes imply some improvements since it usually tends to predict a lower temperature profile, but this approach is often unfit for buoyancy affected cases. At the moment, to the authors' best knowledge, there are no effective techniques for these situations.

The considered model reports underestimation of wall temperature when dealing with downward flow conditions; nevertheless, also the commonly used two equation models usually return good results in these conditions. However, according to the authors' experience (Pucciarelli, 2013; Pucciarelli et al., 2015), for *trans*-pseudo-critical conditions, like the ones reported in Fig. 20, the Zhang et al., 2010 turbulence model seems to be the most promising.

4. Sensitivity of data and predictions to boundary conditions

Some sensitivity analyses were performed for experimental conditions that resembled to lay in a sort of transition region between the one for the occurrence of deterioration phenomena and normal heat transfer conditions. In fact, as stated in past works (Pucciarelli, 2013; Pucciarelli et al., 2015), heat transfer deterioration phenomena seem having a threshold behaviour, working conditions exists in which, even very little changes to the model parameters or boundary conditions, may imply large discrepancies between the calculated trends. This is also supported by some experimental results as the ones reported in Figs. 21 and 22.

In particular, Fig. 21 shows the measured wall temperature trend when varying the mass flux for one of the considered water experimental conditions by Watts (1980). As it can be noticed when moving from G = 340 kg/m^2 s to G = 356 kg/m^2 s, with a relative mass flux increase of roughly 4.7%, the measured wall temperature trend completely changes. Possible high sensitivity is even clearer when considering Fig. 22, reporting one of the experimental conditions by Fewster (1976). Here the inlet temperature is varied and when moving from 24.5 to 25 °C the measured trends no more report heat transfer deterioration and shows improved heat transfer.

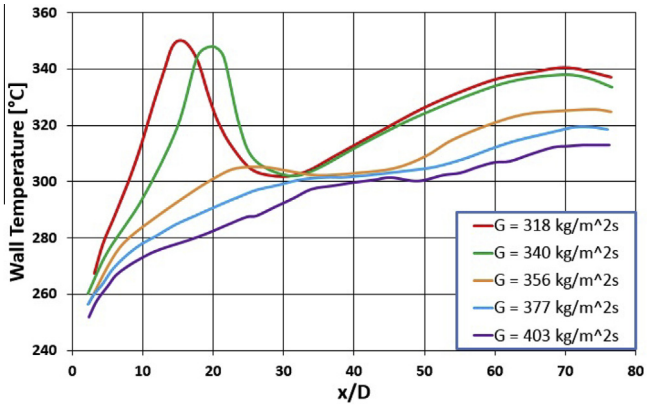

Fig. 21. Data by Watts (1980). Water, 25 MPa, 24.5 mm ID, Tin = 200 °C, q″ = 250 kW/m^2. Measured trends.

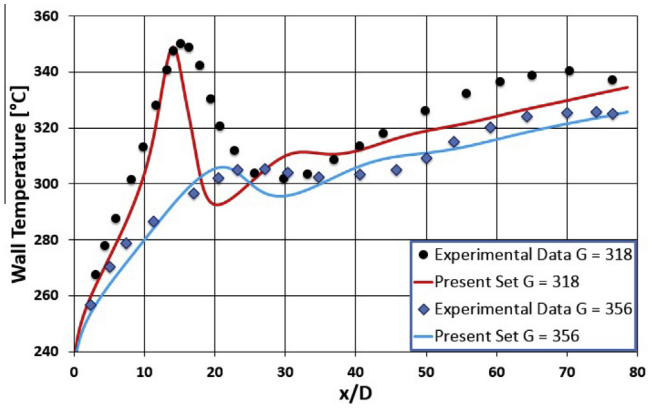

Fig. 23. Data by Watts (1980). Water, 25 MPa, 24.5 mm ID, Tin = 200 °C, q″ = 250 kW/m^2. Results comparison.

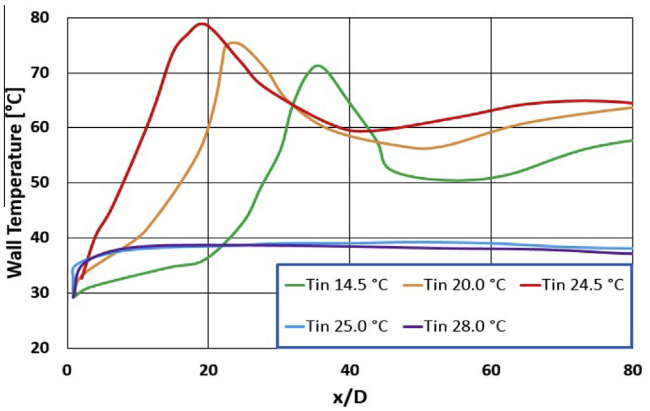

Fig. 22. Data by Fewster (1976). CO_2, 7.584 MPa, 7.88 mm ID, $\dot{m} = 0.02$ kg/s, q″ = 33.6 kW/m^2.

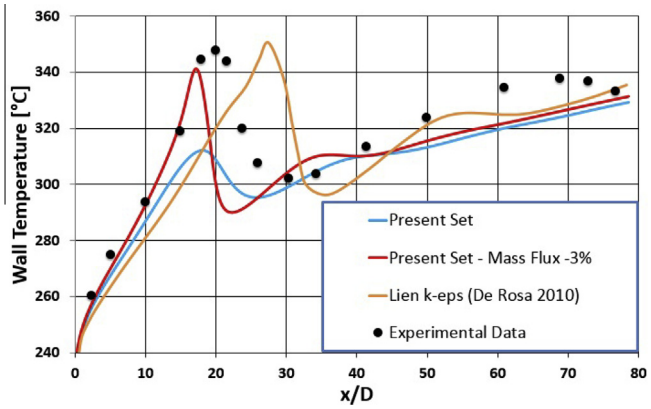

Fig. 24. Data by Watts (1980). Water, 25 MPa, 24.5 mm ID, Tin = 200 °C, G = 340 kg/m^2 s, q″ = 250 kW/m^2.

Consequently, producing good predictions in similar conditions could be very difficult and even slight discrepancies between the nominal and the actual experimental conditions may imply large differences in the obtained trends.

Fig. 23 reports the results obtained when adopting "Present set" for simulating two of the cases reported in Fig. 21. As it can be noticed, the model reproduces quite well the measured trend: nevertheless, some problems arise when considering the conditions in the transition region reported in Fig. 24. The "Present set" reports weak heat transfer deterioration, similar to the one obtained for higher mass fluxes, while higher temperatures were experimentally measured. Consequently, the proposed model seems predicting a thinner and earlier transition region; nevertheless, when decreasing the mass flux of a little amount, such as the considered −3%, improvements are obtained. It must be considered that according to Watts (1980), ±3% is the degree of accuracy of their mass flow measurements, as a consequence the considered condition is plausible.

Uncertainties in the experimental conditions may also affect heat flux. Figs. 25 and 26 report sensitivity analyses concerning the case already mentioned in Fig. 16. First of all, a constant heat flux is imposed all along the heated section; larger changes can be noticed when the flux is increased while no remarkable discrepancies occur when instead decreasing it.

Further analyses were performed adopting a *variable* heat flux along the heated length. Since direct heating was used in performing these experiments, imposed heat flux really depends on the local wall temperature. In fact, as the pipe electrical conductivity

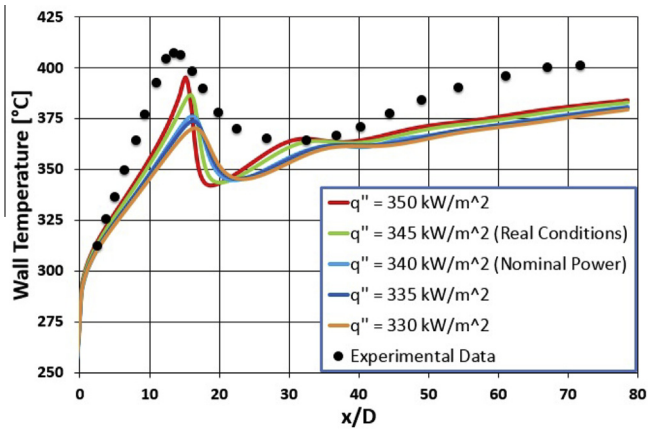

Fig. 25. Data by Watts (1980). Water, 25 MPa, 24.5 mm ID, Tin = 250 °C, G = 392 kg/m^2 s, q″ = 340 kW/m^2. Sensitivity analyses.

decreases with temperature, hotter regions report higher electric resistances, thus increasing the local heat flux. In addition, the azimuthal heat flux distribution may not be uniform, possible differences in the pipe thickness in fact may imply the presence of hotter and colder sides. Watts (1980) reports this information for the considered cases showing that, though the imposed heat flux is 345 kW/m^2 on average, values spanning between 320 kW/m^2 and 350 kW/m^2 are to be considered. Fig. 26 summarises the obtained results showing that a more coherent wall temperature trend may

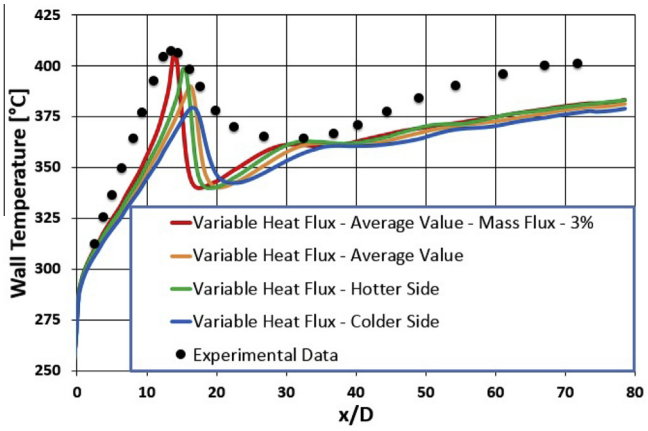

Fig. 26. Data by Watts (1980). Water, 25 MPa, 24.5 mm ID, Tin = 250 °C, G = 392 kg/m^2 s, q″ = 340 kW/m^2. Sensitivity analyses.

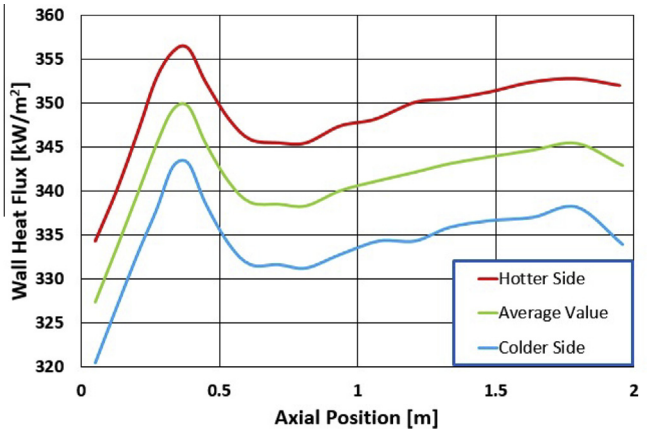

Fig. 27. Data by Watts (1980). Water, 25 MPa, 24.5 mm ID, Tin = 250 °C, G = 392 kg/m^2 s, q″ = 340 kW/m^2. Imposed heat flux trend as reported by Watts.

be achieved by changing the heat flux while remaining inside the uncertainty range of the imposed experimental conditions; Fig. 27 reports instead the imposed heat flux trends. Consequently, at least in cases where buoyancy forces lead the heat transfer phenomenon, the proposed model seems reporting a promising accuracy. No perfect results can be obtained, in such complex conditions; nevertheless, the model seems finally capable to reproduce correctly enough the measured trend both from a qualitative and a quantitative point of view.

Fig. 28 shows results obtained for the sensitivity analysis regarding the experimental conditions by Fewster (1976) summarised in Fig. 22. As it can be noticed the calculated trends still predict an initial heat transfer deterioration even for higher temperatures; consequently, the transition region in this case is much wider and occurs later than in the experimental evidence. Heat transfer deterioration decreases when inlet temperature approaches the pseudo-critical value (T_{pc} = 32.21 °C); improved heat transfer occurs for T_{in} = 32 °C while normal heat transfer happens for higher temperatures.

Dealing with bulk conditions very close to the pseudo-critical temperature is in fact very challenging for turbulence models since the whole fluid, not just the one close to the wall region, undergoes strong properties changes. RANS Turbulence models often return bad predictions in these cases, probably because the time-averaging operation and the considered closure relations do not allow them representing the strongly turbulent phenomena that surely occur in those conditions. Consequently, instead of

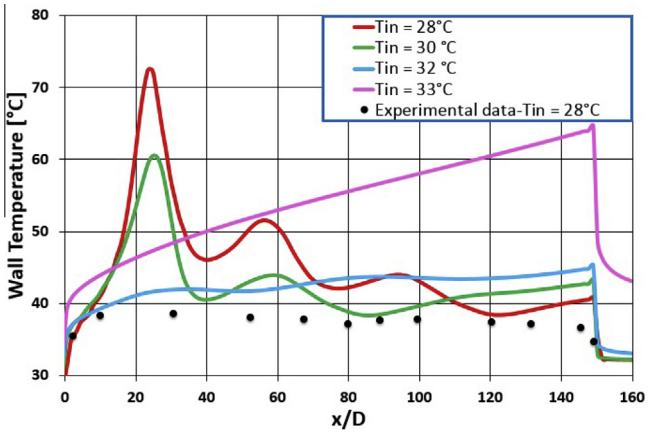

Fig. 28. Data by Fewster (1976). CO_2, 7.584 MPa, 7.88 mm ID, $\dot{m}$ = 0.02 kg/s, q″ = 33.6 kW/m^2 inlet temperature sensitivity analyses.

predicting improved heat transfer, they return heat transfer deterioration due to the worsening of the heat transfer properties.

As for the case reported in Fig. 19 for the data by Ornatskiy, problems still hold in achieving good predictions. If the main reason of these discrepancies is due an underestimation of turbulence, as supposed above, a possible path for the resolution could be introducing an additional empirical turbulence production term accounting for missing effects.

5. Conclusions

The main goal of the present paper was improving the predictions obtained with RANS turbulence models when dealing with fluids at supercritical pressure. Moving from previous assumptions, a new definition for the $1 - C_{t3}$ quantity from the AHFM equation is proposed showing promising results. Instead of considering a constant value as in past works, a relation taking into account the dimensionless enthalpy is adopted. The approach should allow considering the proposed definition even when dealing with different fluids as suggested from parallel works concerning fluid to fluid scaling. As a first conclusion, it must be noted that this approach resulted quite successful in a variety of addressed cases, involving different fluids and operating conditions.

In the present paper the turbulent heat flux evaluated by the AHFM is used also in the energy equation, as an advanced rationale for calculating the turbulent Prandtl number, in addition to its use for evaluating the buoyancy terms in turbulence production. This approach was already introduced in the frame of a previous paper (Pucciarelli et al., 2016), highlighting a potential for improvement in model performance for small pipe sizes, being less satisfactory for larger ones. This was mainly due to the constant value adopted for the $1 - C_{t3}$ parameter.

Sensitivity analyses were also performed for some transition regions where, as reported in the previous sections, the heat transfer deterioration phenomenon seems showing a threshold behaviour; consequently, working conditions exist where *even little changes in the boundary conditions imply very large changes* in the obtained temperature trend.

The adopted model reported promising results in analysing the mass flux effect in conditions far from the pseudo-critical temperature, while definitively poorer predictions were obtained considering the inlet temperature influence, at least in the addressed cases. Nevertheless, the limited success in the former case is mainly due to the fact that inlet conditions are very close to the pseudo-critical temperature, a situation which proved to be very difficult to deal with even in past works.

Problems still hold for downward flow cases and for the ones with large mass fluxes in trans pseudo-critical conditions. Nevertheless, the former operating conditions do not represent a big issue, since turbulence models returning good predictions for downward flow already exist and need little improvement; nevertheless, attempts for improving the results obtained by the model proposed in this paper also for downward flow should be performed in the future, in order to achieve good predictions for all the relevant operating conditions by a single turbulence model.

It must be finally remarked that the above results have been obtained considering a quite representative range of fluids and operating conditions; this demonstrates that the proposed technique does not work only for single selected cases, but for many possible conditions explored in available experimental data.

Acknowledgments

The IAEA is acknowledged for including the present research in the Coordinated Research Project on "Understanding and Prediction of Thermal-Hydraulics Phenomena Relevant to SCWRs" through the IAEA Research Agreement No: 18425/R0.

CD-Adapco is also acknowledged for making possible this work.

References

Abe, K., Kondoh, T., Nagano, Y., 1994. A new turbulence model for predicting fluid flow and heat transfer in separating and reattaching flows—I. Flow field calculations. Int. J. Heat Mass Transfer 37 (1), 139–151.

Abe, K., Kondoh, T., Nagano, Y., 1995. A new turbulence model for predicting fluid flow and heat transfer in separating and reattaching flows—II. Thermal field calculations. Int. J. Heat Mass Transfer 38 (8), 1467–1481.

Ambrosini, W., Sharabi, M., 2008. Dimensionless parameters in stability analysis of heated channels with fluids at supercritical pressures. Nucl. Eng. Des. 238 (2008), 1917–1929. Also published at ICONE-14 in 2006.

Ambrosini, W., Pucciarelli, A., Borroni, I., 2015. A methodology for including wall roughness effects in k-ε low Reynolds turbulence models. Part I: basis of the methodology. Nucl. Eng. Des. 286 (2015), 175–194.

Badiali, S., 2011. Numerical investigation using CFD codes of heat transfer with fluids at supercritical pressure (MSc thesis). Dipartimento di Ingegneria Meccanica, Nucleare e della Produzione, Università di Pisa, Pisa, Italy.

Bae, J.H., Yoo, J.Y., Choi, H., 2005. Direct numerical simulation of turbulent supercritical flows with heat transfer. Phys. Fluids 17.

Borroni, I., 2014. Analysis by CFD models of deterioration heat transfer phenomena for supercritical fluids (MSc thesis). Dipartimento di Ingegneria dell'Energia, dei Sistemi, del Territorio e delle Costruzioni, University of Pisa, Italy.

CD-adapco, 2015. USER GUIDE STAR-CCM+ Version 10.06.010.

De Rosa, M., 2010. Computational fluid-dynamic analysis of experimental data on heat transfer deterioration with supercritical water (MSc thesis). Department of Mechanical Engineering and Nuclear, University of Pisa, Italy.

Fewster, J., 1976. Mixed forced and free convective heat transfer to supercritical pressure fluids flowing in vertical pipes (PhD thesis). University of Manchester.

Jackson, J.D., Hall, W.B., 1979. Forced Convection Heat Transfer to Fluids at Supercritical Pressure in Turbulence Forced Convection in Channels and Bundles. Hemisphere Publishing Corporation, Manchester, pp. 563–611.

Kenjereš, S., Gunarjo, S.B., Hanjalić, K., 2005. Contribution to elliptic relaxation of turbulent and natural mixed convection. Int. J. Heat Fluid Flow 26, 569–586.

Launder, B.E., 1987. An introduction to single-point closure methodology complex turbulent flows. An Introduction to the Modelling of Turbulence, Lecture Series 1987–06, Von Karman Inst. For Fluid Dynamics, Rhode-Saint-Genese, Belgium (also available as UMIST Mech. Eng. Dept. Report TFD/87/7).

Launder, B.E., 1988. On the computation of convective heat transfer in complex turbulent flows. J. Heat Transfer 110/1113.

Lien, F.S., Chen, W.L., Leschziner, M.A., 1996. Low-Reynolds number eddy viscosity modelling based on non-linear stress-strain/vorticity relations. In: Proceedings of the 3rd Symposium on Engineering Turbulence Modelling and Measurements, 27–29 May, Crete, Greece.

Menter, F.R., 1994. Two-equation eddy-viscosity turbulence modelling for engineering applications. AIAA J. 32 (8), 1598–1605.

Ornatsky, A.P., Glushchenko, L.P., 1971. Heat transfer with rising and falling flows of water in tube of small diameter at supercritical pressures. Therm. Eng., 137–141

Pis'menny, E.N., Razumovskiy, V.G., Maevskiy, E.M., Kotoskov A.G., Pioro I.L., 2005. Heat transfer to supercritical water in gaseous state or affected by mixed convection in vertical tubes. In: Proceedings of ICONE14 "International Conference of Nuclear Engineering". Miami, Florida, USA.

Pis'menny, E.N., Razumovskiy, V.G., Maevskiy, E.M., 2005. Experimental study on temperature regimes to supercritical water flowing in vertical tubes at low mass fluxes. In: Proceedings of the International Conference GLOBAL-2005 Nuclear Energy Systems for Future Generation and Global Sustainability, Tsukuba, Japan, October 9–13, paper no. 519.

Pucciarelli, A., 2013. Analysis of heat transfer phenomena with supercritical fluids by four equation turbulence models (MSc thesis). Dipartimento di Ingegneria dell'Energia, dei Sistemi, del Territorio e delle Costruzioni, University of Pisa, Italy.

Pucciarelli, A., Ambrosini, W., 2016. Fluid-to-fluid scaling of heat transfer phenomena with supercritical pressure fluids: results from RANS analyses. Ann. Nucl. Energy 92 (2016), 21–35.

Pucciarelli, A., Borroni, I., Sharabi, M., Ambrosini, W., 2015. Results of 4-equation turbulence models in the prediction of heat transfer to supercritical pressure fluids. Nucl. Eng. Des. 281 (2015), 5–14.

Pucciarelli, A., Sharabi, M., Ambrosini, W., 2016. Improving the prediction of heat transfer to supercritical fluids in upword flow cases by CFD models. Nucl. Eng. Des. 297 (2016), 257–266.

Shams, A., Roelofs, F., Baglietto, E., Lardeau, S., Kenjeres, S., 2014. Assessment and calibration of an algebraic turbulent heat flux model for low-Prandtl fluids. Int. J. Heat Mass Transfer 79 (2014), 589–601.

Sharabi, M.B., 2008. CFD analyses of heat transfer and flow instability phenomena relevant to fuel bundles in supercritical water reactors (Research Doctorate thesis). Università di Pisa.

Sharabi, M.B., Ambrosini, W., 2009. Discussion of heat transfer phenomena in fluids at supercritical pressure with the aid of CFD models. Ann. Nucl. Energy 36 (2009), 60–71.

Watts, M.J., 1980. Heat transfer to supercritical pressure water – mixed convection with upflow and downflow in a vertical tube (PhD thesis). University of Manchester.

Xiong, J., Cheng, X., 2014. Turbulence modelling for supercritical pressure heat transfer in upward flow tubes. Nucl. Eng. Des. 270, 249–258.

Zhang, H., Xie, Z.R., Yang, Y.H. 2010. Numerical study on supercritical fluids and heat transfer under buoyancy. In: The 8th International Topical Meeting on Nuclear Thermal-Hydraulics, Operation and Safety (NUTHOS-8), Shanghai, China, October 10–14, 2010.